

TextCrafter: Accurately Rendering Multiple Texts in Complex Visual Scenes

Nikai Du^{1,†}, Zhenan Chen^{1,†}, Shan Gao², Zhizhou Chen¹
Xi Chen², Zhengkai Jiang³, Jian Yang¹, Ying Tai^{1,§}

¹Nanjing University

²China Mobile

³The Hong Kong University of Science and Technology
502024710004@smail.nju.edu.cn

Project Page: <https://github.com/NJU-PCALab/TextCrafter.git>

[†]Equal contribution, [§]Corresponding author

Abstract

This paper explores the task of Complex Visual Text Generation (CVTG), which centers on generating intricate textual content distributed across diverse regions within visual images. In CVTG, image generation models often rendering distorted and blurred visual text or missing some visual text. To tackle these challenges, we propose TextCrafter, a novel multi-visual text rendering method. TextCrafter employs a progressive strategy to decompose complex visual text into distinct components while ensuring robust alignment between textual content and its visual carrier. Additionally, it incorporates a token focus enhancement mechanism to amplify the prominence of visual text during the generation process. TextCrafter effectively addresses key challenges in CVTG tasks, such as text confusion, omissions, and blurriness. Moreover, we present a new benchmark dataset, CVTG-2K, tailored to rigorously evaluate the performance of generative models on CVTG tasks. Extensive experiments demonstrate that our method surpasses state-of-the-art approaches.

Introduction

In recent years, diffusion models (Ho, Jain, and Abbeel 2020; Podell et al. 2023; Rombach et al. 2022; Ramesh et al. 2021, 2022; Zhao et al. 2024; Dhariwal and Nichol 2021; Chen et al. 2023) have emerged as the forefront technology in image generation. Recent studies, represented by general-purpose text-to-image models such as FLUX (BlackForest 2024) and SD 3 (Esser et al. 2024), have acquired the ability to render simple visual text through large-scale pretraining. However, when confronted with complex real-world visual text scenarios, these models often struggle with critical challenges such as text distortion, omission, and blurriness. These shortcomings significantly hinder their practical applicability in real-world use cases. Achieving precise, legible, and contextually accurate visual text rendering in complex scenes remains essential yet highly challenging.

Recent studies in multi-instance generation (Feng et al. 2022; Zhou et al. 2024; Chen et al. 2024b; Zhou et al. 2025b) primarily focus on generating multiple instances within a single image simultaneously, striving to achieve precise regulation over factors such as quantity, position and attributes. However, a crucial yet often overlooked category in the visual domain is visual text. Text is an indispensable component of the real world, distinguished by its unparalleled

complexity and delicacy compared to conventional objects, flora, or fauna. Unlike these entities, text possesses an exceptionally intricate internal structure, where even minor alterations can cause significant changes in visual appearance, potentially leading to misrecognition or complete illegibility. Existing multi-instance generation approaches, such as MIGC (Zhou et al. 2024) and 3DIS (Zhou et al. 2025b), primarily focus on sentence-level information and interaction, offering a limited understanding of text at a finer granularity. Moreover, RPG (Yang et al. 2024a) and RAG-Diffusion (Chen et al. 2024b) adjust instance structures during attention fusion but fall short of the precision and stability needed for visual text rendering.

Recent studies on visual text rendering primarily focus on accurately generating a *single* text region. For instance, methods like AnyText (Tuo et al. 2024), Glyph-byT5 (Liu et al. 2025), SceneTextGen (Zhangli et al. 2024), Diff-Text (Zhang et al. 2024b), and TextDiffuser (Chen et al. 2024a) often employ specialized modules to encode visual text representations and condition the diffusion model accordingly. However, these methods face two major limitations: 1) They rely on predefined rules to synthesize visual text training datasets. Due to the need for highly accurate text annotations, manual verification is often required, making the creation of complex visual text datasets both *labor-intensive and costly*. 2) Most approaches depend on fine-tuned text encoders (*e.g.*, Glyph-by-T5) or trained conditional control encoders (*e.g.*, AnyText, TextDiffuser, SceneTextGen) to facilitate text generation. In complex multi-text generation, however, these approaches often cause interference among the control features of different targets, making it difficult to balance *fine-grained local control with global consistency across multiple texts*.

This paper explores the task of Complex Visual Text Generation (CVTG), which aims to generate intricate text content distributed across different regions. To tackle the challenges of CVTG, we propose TextCrafter, a novel *training-free* framework for rendering multiple texts in complex visual scenes. TextCrafter enhances multi-text control, ensuring accurate text presentation and logical layout. Our framework comprises three key stages: 1) **Instance Fusion**: This stage strengthens the connection between visual text and its corresponding carrier, ensuring strong consistency between

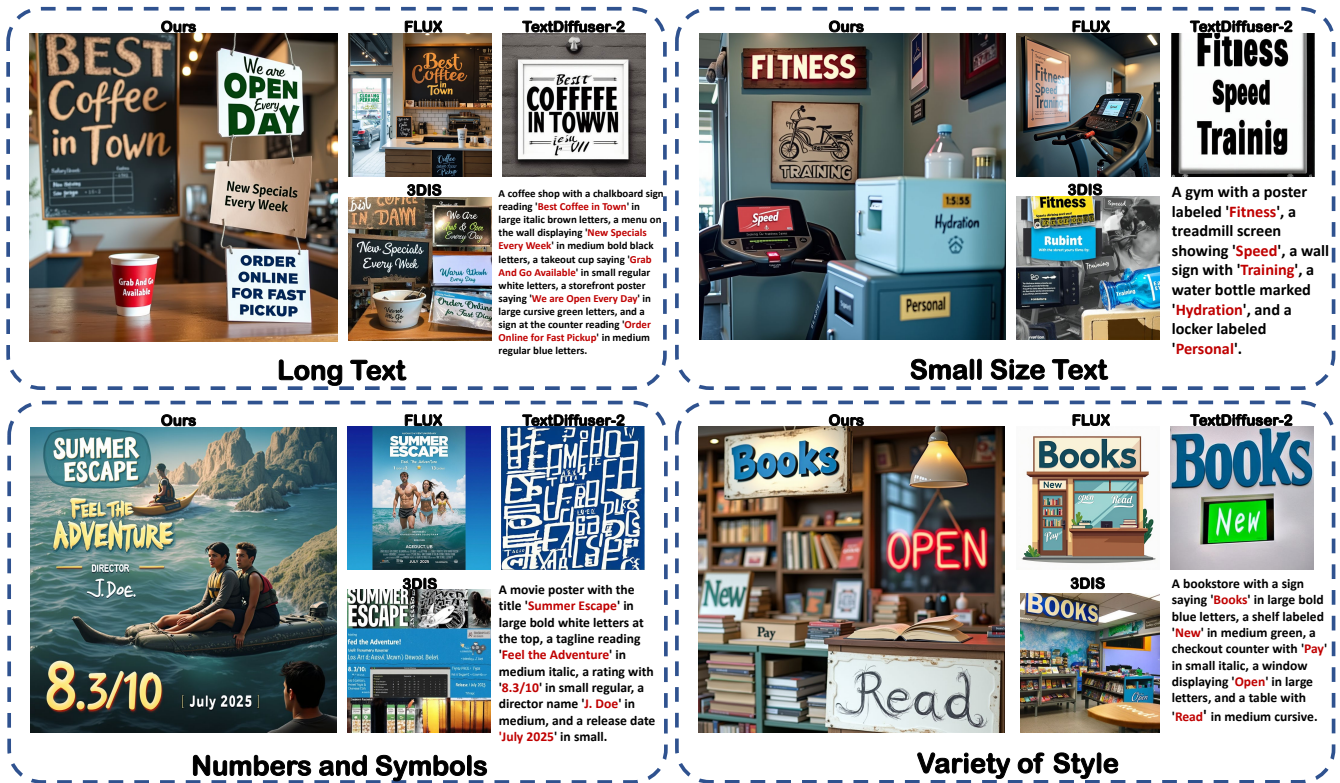


Figure 1: TextCrafter enables precise multi-region visual text rendering, addressing the challenges of long, small-size, various numbers, symbols and styles in visual text generation. We illustrate the comparisons among TextCrafter with three state-of-the-art models, *i.e.*, FLUX (BlackForest 2024), TextDiffuser-2 (Chen et al. 2025) and 3DIS (Zhou et al. 2025b).

the text content and its surrounding environment. It effectively prevents text from appearing in *incorrect positions*. 2) **Region Insulation**: Leveraging the positional priors of the pre-trained DiT model (Peebles and Xie 2023), this step initializes the layout information for each text instance while separating and denoising text prompts across different regions. This process prevents early interference between text areas, *reducing confusion and the risk of content omission* in multi-text scenarios. 3) **Text Focus**: An attention control mechanism is introduced to enhance the attention maps of visual text, refining the fidelity of text rendering. This stage ensures *textual accuracy* and addresses issues of *blurriness, particularly in smaller text*. We present some examples in Figure 1. Our contributions are summarized as follows:

- We propose TextCrafter, a novel *training-free* framework for rendering multiple texts in complex visual scenes, consisting of three key stages: Instance Fusion, Region Insulation, and Text Focus.
- We construct a new CVTG-2K dataset, which encompasses a diverse range of visual text prompts varying in position, quantity, length, and attributes, serving as a robust benchmark for evaluating the performance of generation models in CVTG tasks.
- We conduct extensive quantitative and qualitative experiments on the CVTG-2K and an established benchmark. The results demonstrate that TextCrafter exhibits superior

effectiveness and robustness in the CVTG task.

Related Works

Compositional Generation and Multi-instance Generation. Attend-and-Excite (Chefer et al. 2023) and BOX-Diffusion (Xie et al. 2023) guide pre-trained diffusion models to align generated instances with prompts. GLIGEN (Li et al. 2023), MIGC (Zhou et al. 2024), and CreativeLayout (Zhang et al. 2024a) enhance control by incorporating bounding box conditions into trainable layers. RPG (Yang et al. 2024a), RAG-Diffusion (Chen et al. 2024b) and DreamRenderer (Zhou et al. 2025a) break the generation process into regional tasks for compositional generation. However, these methods often overlook a critical kind of instance: *visual text*, as a key component of visual scenes.

Visual Text Generation. DiffSTE (Ji et al. 2023), GlyphByT5 (Liu et al. 2025), and UDiffText (Zhao and Lian 2025) use character-level encoders to incorporate word appearance into embeddings. TextDiffuser (Chen et al. 2024a) creates text layout masks for injection into the latent space. Approaches like Diff-Text (Zhang et al. 2024b) improve text accuracy with attention map restrictions. GlyphDraw (Ma et al. 2023) uses two models for text position prediction and rendering. TextDiffuser-2 (Chen et al. 2025) leverages large language models for layout planning. However, these

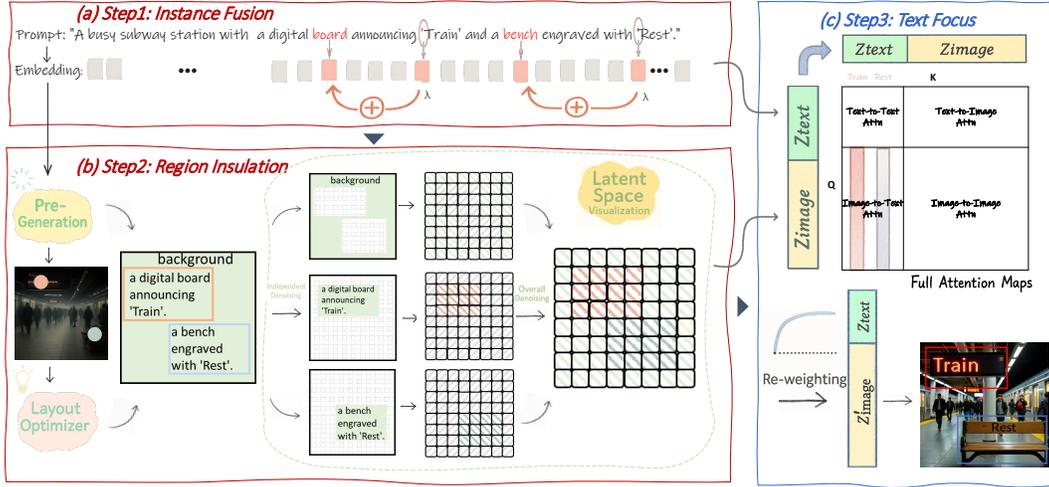


Figure 2: **Overview of our TextCrafter.** TextCrafter consists of three steps. (a) *Instance Fusion*: strengthen the connection between visual text and its corresponding carrier. (b) *Region Insulation*: leverage the positional priors of the pre-trained DiT model to initialize the layout information for each text instance while separating and denoising text prompts across different regions. (c) *Text Focus*: enhance the attention maps of visual text, refining the fidelity of text rendering.

approaches often optimize text rendering for *single region*, leading to poor generalization in complex visual text scenes.

Benchmark for Visual Text Generation. Earlier works like GlyphControl introduced SimpleBench and CreativeBench (Yang et al. 2024b), but these fixed-template datasets offer limited diversity and contain only single-word scenes. MARIO-Eval (Chen et al. 2024a) suffers from low-quality prompts and unclear semantics. Although DrawText (Ma et al. 2023) collects prompts for generating natural scenes, the comprehensiveness and scale of the dataset are insufficient. AnyText-benchmark (Tuo et al. 2024) allows multi-word prompts but treats each word separately and appends them directly to the caption, limiting data distribution. Existing visual text benchmarks focus on text generation within *a single object or location*, falling short of capturing the complexity of real-world scenes. Thus, we propose a benchmark CVTG-2K to incorporate *diverse positions, quantities, lengths, and attributes* for comprehensively evaluate models in complex visual text scenarios.

Methodology

Overview

Problem Definition. In CVTG, users provide a global prompt P containing multiple visual text descriptions $D = \{d_1, d_2, \dots, d_n\}$, where each description includes the visual text’s content and descriptors (position, attributes). The visual texts’ content are defined as $VT = \{vt_1, vt_2, \dots, vt_n\}$, with each vt_i corresponding to description d_i . The model must generate an image from prompt P where each vt_i appears with its corresponding description d_i .

Challenges in CVTG. Complex prompts cause interference among visual texts, leading to three degradation issues:

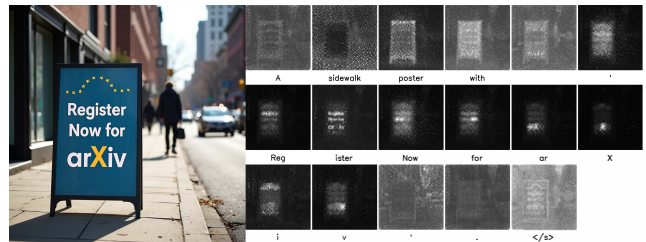


Figure 3: **Illustration of tokenizing the prompt** “A sidewalk poster with ‘Register Now for arXiv.’” along with the attention map corresponding to each token. The use of preceding quotation marks can reinforce the relationship between text tokens and carrier tokens.

- 1) *Text confusion*: Visual texts vt_i and vt_j intertwine, generating erroneous characters/words.
- 2) *Text omission*: Only text from description d_i appears, neglecting vt_j from d_j .
- 3) *Text blurriness*: Small-scale text in d_i receives insufficient attention, appearing blurred in the generated image.

Motivation. Current text-to-image models excel with individual visual texts. By decomposing CVTG into simpler sub-tasks, overall complexity decreases. Solving these sub-tasks separately and combining their solutions accomplishes the CVTG task. This approach shifts focus progressively from the entire task to sub-tasks then to specific visual texts, enabling precise rendering. Based on this coarse-to-fine strategy, we present TextCrafter (Figure 2).

Novelty. TextCrafter differs significantly from existing compositional generation and multi-instance generation (collectively referred to as MIC) methods. MIC methods excel at generating multiple instances of different categories, but often suffer from feature interference when handling

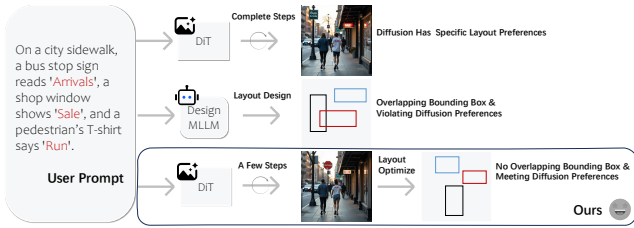


Figure 4: **Motivation for layout optimizer.** LLM/MLLM-based layout designers frequently generate overlapping bounding boxes, which do not align with the layout preferences of Diffusion models. Our proposed layout optimizer addresses this limitation without additional fine-tuning.



Figure 5: **For a pre-trained DiT model, only a few denoising steps are required to approximate the image layout and subject positions.** After 8 steps, the layout closely resembles that of a full 50-step process, with subsequent iterations primarily refining details.

highly similar instances, leading to corruption of internal instance structure. TextCrafter addresses this issue through a dual mechanism: while MIC methods treat each instance as an independent entity during generation, TextCrafter employs Instance Fusion to bind text instances with their visual carriers, subsequently treating them as unified wholes during generation, thereby enhancing distinctions between different text instances. Additionally, the MILP layout optimizer generates non-overlapping layouts through hard constraints, eliminating overlapping regions. Overlapping or mutually contained regions are extremely common in MIC tasks, highlighting an inherent difference between MIC and CVTG tasks. By separating the latent spaces of text instances from the initial generation stage, Region Insulation fundamentally prevents feature leakage caused by content similarity.

Instance Fusion

It is crucial to prevent visual texts from floating on the surface and ensure proper positioning. We propose an Instance Fusion strategy that integrates the visual text’s content with its spatial carrier. Rather than using the text’s own embedding, we leverage embedding of the preceding quotation mark to establish spatial relationships. As illustrated in Figure 3, the preceding quotation mark in the attention map corresponds to the visual text it governs, indicating that it encapsulates complete information about the text. According to token additivity (Hu et al. 2024), we incorporate the preceding quotation mark’s embedding into the carrier’s embedding via weighted fusion to ensure precise alignment, where λ controls the proportion of the addition.

Benchmark	Num	Word	Char	Attribute	Region
CreativeBench	400	1.00	7.29	×	×
MARIOEval	5414	2.92	15.47	×	×
DrawTextExt	220	3.75	17.01	×	×
AnyText-benchmark	1000	4.18	21.84	×	×
CVTG-2K	2000	8.10	39.47	size/color/ font ✓	2/3/4/5 ✓

Table 1: **Comparison of CVTG-2K with existing public visual text Benchmarks** in terms of Number of Samples (Num), Average Word Count (Word), Average Character Count (Char), Attribute, and number of Regions (Region).

Region Insulation

Pre-generation. In CVTG, multiple texts often influence each other’s glyphs and layout (Zheng et al. 2023). To simplify, we decouple them into independent instances. Specifically, we assign a rectangular bounding box to each visual text to represent its layout. This allows us to effectively isolate the texts, preventing interference during generation. Instead of manually specifying layouts or relying on MLLMs, we leverage the diffusion model’s learned positional knowledge (Tumanyan et al. 2023). Figure 4 demonstrates a notable limitation of MLLMs: despite dedicated fine-tuning, the layouts they provide often exhibit overlapping bounding boxes and do not conform to the layout preferences inherent in Diffusion models. As shown in Figure 5, during the early denoising steps, we capture attention maps and identify the points of maximum attention for each visual text. This pre-generation process guides layout initialization. Assume that the attention map obtained during this process is A_t , where t represents the current step, and p stands for pixel:

$$p_{\max} = \arg \max_p A_t(p). \quad (1)$$

Layout Optimizer. Next, the rectangular bounding boxes for each visual text are optimized using Mixed-Integer Linear Programming (MILP) to minimize the Manhattan distance (L1 norm) between the bounding box center and the maximum attention point. Let $p_{\max,i}$ be the maximum attention point of vt_i and $p_{\text{center},i}$ the rectangular bounding box center. Thus, the optimization objective is:

$$\min \sum_{i=1}^n |p_{\text{center},i} - p_{\max,i}|_1 \quad (2)$$

Additionally, we enforce constraints on the *minimum area*, *aspect ratio*, and *non-overlapping* properties of the bounding boxes. Further details of the MILP optimizer can be found in the Supplementary Material. The solution to this optimization problem can be represented as assigning a bounding box bbx_i ($m_{\text{offset}}, n_{\text{offset}}, m_{\text{scale}}, n_{\text{scale}}$) to each description d_i . Then, we encode the prompt P and the corresponding descriptions of visual text $D = \{d_1, d_2, \dots, d_n\}$, obtaining values for c and $\{\hat{c}^1, \hat{c}^2, \dots, \hat{c}^n\}$. c needs to be processed through Instance Fusion. The latent \hat{x}_i is conditioned on \hat{c}_i , and the initial latent x is conditioned on the

Model	Word Accuracy \uparrow	NED \uparrow	CLIPScore \uparrow	VQAScore \uparrow	Aesthetics \uparrow
FLUX.1 dev [2024]	0.4965	0.6879	0.7401	0.8886	5.91
SD3.5 Large [ICML 2024]	0.6548	0.8470	0.7797	<u>0.9297</u>	5.56
AnyText [ICLR 2024]	0.1804	0.4675	0.7432	0.6935	4.53
TextDiffuser-2 [ECCV 2024]	0.2326	0.4353	0.6765	0.5627	4.51
RAG-Diffusion [ICCV 2025]	0.2648	0.4498	0.6688	0.6397	5.58
3DIS [ICLR 2025]	0.3813	0.6505	0.7767	0.8684	4.86
TextCrafter (FLUX)	<u>0.7370</u>	<u>0.8679</u>	<u>0.7868</u>	0.9140	<u>5.70</u>
TextCrafter (SD3.5)	0.7600	0.9038	0.8023	0.9299	5.45

Table 2: **Quantitative results on CVTG-2K dataset.** Bold values denote the best performance, while underlined values indicate the second-best performance for each metric.

complete c . When $t > T - r$ (i.e., during the first r steps of the denoising process), denoising follows the formula:

$$x_{t-1} = x_t - \epsilon_\theta(x_t, c), \quad \hat{x}_{t-1}^i = \hat{x}_t^i - \epsilon_\theta(\hat{x}_t^i, \hat{c}^i) \quad (3)$$

where ϵ_θ represents the noise predictor. After each denoising step, \hat{x}_t^i is reinserted into the corresponding region in x_t .

Text Focus

Region Insulation creates distinct visual boundaries between visual texts. To enhance harmony, regions are merged into a single latent variable for denoising, but this may blur smaller texts. To preserve structure, we boost attention scores (Hertz et al. 2022) for texts and preceding quotation marks, capping enhancement at $2\times$ to prevent overamplification. To ensure control, we employ the tanh function. The k token sequence is denoted as $F = \{f_1, \dots, f_k\}$. The enhancement ratio is:

$$\text{ratio} = 1 + \tanh(0.5 \cdot k). \quad (4)$$

We use a smaller ratio for single-word cases. Unlike UNet’s cross-attention, MM-DiT employs a full attention matrix with four regions: image-to-image, text-to-text, text-to-image, and image-to-text (Cai et al. 2024). We re-weight the image-to-text matrix, which controls image modality and enhances focus on visual text. At step t , the operation for each element in M_t is expressed as:

$$\text{Focus}(M_t)_{i,j} = \begin{cases} \text{ratio} \cdot (M_t)_{i,j} & \text{if } j \in F \\ (M_t)_{i,j} & \text{otherwise.} \end{cases} \quad (5)$$

The overall algorithm is illustrated in Algorithm 1.

Experiments

Benchmark

CVTG-2K. Currently, there is a lack of publicly available benchmark datasets specifically designed for complex visual text generation tasks. Therefore, we propose CVTG-2K, a challenging public benchmark dataset for complex visual text. All prompts are generated through the OpenAI’s O1-mini API (OpenAI 2024). These prompts encompass a variety of scenes containing complex visual texts, including but not limited to street views, book covers, advertisements, posters, notes, memes, logos, and movie frames. Unlike previous standard datasets synthesized using fixed rules,



Figure 6: **Qualitative comparison of TextCrafter with other baselines on CVTG-2K.** TextCrafter excels in delivering harmonious and aesthetically pleasing images. It also accurately renders multiple visual texts while maintaining stability in complex scenarios.

CVTG-2K ensures the diversity and rationality of the data distribution. We first prompt the O1 model to conceive a scene and then imagine the possible visual texts that may appear in that scene, utilizing Chain-of-Thought (CoT) (Wei et al. 2022) techniques to ensure the quality of the generated prompts. For further details on the dialogue template with O1, refer to the supplementary material. Through rigorous filtering rules and meticulous post-processing, we have generated 2,000 prompts containing complex visual texts. On average, the visual texts in CVTG-2K contain 8.10 words and 39.47 characters, surpassing all previously published visual text benchmark datasets in terms of visual text length. Table 1 presents a comparison of the data in CVTG-2K with currently available benchmark datasets. Furthermore, CVTG-2K is the first benchmark dataset to include the number of multiple visual text regions, with the number of regions ranging from 2 to 5. We have assigned different proportions to these region numbers, approximately 20%, 30%, 30%, and 20%. With its diverse region numbers and visual text lengths, CVTG-2K provides a comprehensive evaluation of model performance in complex visual text generation. Through careful review, CVTG-2K ensures that it does not contain any discriminatory or inflammatory content.

To further enhance the challenge of CVTG-2K, we randomly added attributes to each visual text in half of the data.

Algorithm 1: TextCrafter Image Generation

```

1: Input: The encoded embedding of a global prompt  $P$  is denoted as  $c$ . The encoded embedding of multiple descriptions  $D$  is denoted as  $\{\hat{c}^1, \hat{c}^2, \dots, \hat{c}^n\}$ .
2: Parameter: the proportion of the addition  $\lambda$ , the  $r$  steps of Region Insulation, the pre-generation steps  $\tau$ .
3: Output: A generated latent  $x_0$ 
4: {Step 1: Instance Fusion}
5:  $c = \text{InstanceFusion}(c, \lambda)$ 
6: {Step 2: Region Insulation}
7:  $z_t \sim \mathcal{N}(0, 1)$ 
8: for  $t = \tau, \tau - 1, \dots, 1$  do
9:    $z_{t-1}, A_t \leftarrow \text{DiT}(z_t, c, t)$ 
10: end for
11: for  $i = 1, 2, \dots, n$  do
12:    $p_i \leftarrow (0, 0)$ 
13:    $p_{\max, i} \leftarrow \arg \max_{p_i} A_t(p_i, i)$ 
14: end for
15:  $bbx_1, \dots, bbx_n \leftarrow \text{MILP}(p_{\max, 1}, \dots, p_{\max, n})$ 
16:  $x_T \sim \mathcal{N}(0, 1)$ 
17: for  $i = 1, 2, \dots, n$  do
18:    $\hat{x}_t^i \leftarrow \text{Initialize}(\mathcal{N}(0, 1), bbx_i)$ 
19: end for
20: for  $t = T, T - 1, \dots, T - r + 1$  do
21:    $x_{t-1} \leftarrow x_t - \epsilon_\theta(x_t, c)$ 
22:   for  $i = 1, 2, \dots, n$  do
23:      $\hat{x}_{t-1}^i \leftarrow \hat{x}_t^i - \epsilon_\theta(\hat{x}_t^i, \hat{c}^i)$ 
24:      $x_{t-1} \leftarrow \text{Reinsert}(x_{t-1}, \hat{x}_{t-1}^i, bbx_i)$ 
25:   end for
26: end for
27: {Step 3: Text Focus}
28: for  $t = T - r, T - r - 1, \dots, 1$  do
29:   for  $\text{AttentionLayer}_i \in \epsilon_\theta$  do
30:      $M_t = Q_t^i \times K_t^i$ 
31:      $M_t \leftarrow \text{Focus}(M_t)$ 
32:      $\text{Attention}_t^i \leftarrow \text{softmax}(M_t / \sqrt{d}) \times V_i$ 
33:   end for
34:    $x_{t-1} \leftarrow x_t - \epsilon_\theta(x_t, c)$ 
35: end for
36: return  $x_0$ 

```

The attributes include size, color, and font. The sizes are categorized as large, medium, and small, and the fonts include regular, bold, italic, and cursive. All attributes are labeled using natural language to ensure that the text encoder can process them without the need for special designs. Each visual text will randomly have one or more of these attributes. This design will promote further research into the stylization and customization of visual texts in future studies. Additionally, we provide more fine-grained information. We decouple the prompts using O1-mini, separating descriptions $D = \{d_1, d_2, \dots, d_n\}$ containing multiple visual texts and expressing the relationship between each visual text and its position through the most critical words, which is the carrier of the visual text. Through meticulous manual review, we ensured the accuracy of this fine-grained information. CVTG-2K has been publicly released alongside our code, and the dataset is available for any users adhering to the usage guidelines. For more examples of CVTG-2K, please refer to the supplementary material.

Metric	AnyText	TextDiffuser-2	TextCrafter
Word Accuracy \uparrow	0.1301	<u>0.5466</u>	0.6972
NED \uparrow	0.4401	<u>0.7849</u>	0.8855
CLIPScore \uparrow	0.7352	0.8240	<u>0.8181</u>
VQAScore \uparrow	0.7037	0.8669	<u>0.8607</u>
Aesthetics \uparrow	3.39	<u>3.49</u>	4.39

Table 3: **Quantitative results on MARIOEval subset** (Chen et al. 2024a). Bold values denote the best performance, while underlined values indicate the second-best performance for each metric.

Steps	Word Accuracy \uparrow	NED \uparrow
Step1(Instance Fusion)	0.4422	0.6495
Step2(Region Insulation)	0.6116	0.7750
Step3(Text Focus)	0.6351	0.8055
Step1+Step2	0.6121	0.7762
Step2+Step3	0.7328	0.8651
All	0.7370	0.8679
Layout Methods	Word Accuracy \uparrow	NED \uparrow
Random	0.6900	0.8374
Fixed	0.6994	0.8475
Optimizer	0.7370	0.8679

Table 4: **Ablation studies** on CVTG-2K dataset

MARIOEval. To supplement our evaluation of TextCrafter’s applicability in single-text and simple-scene scenarios, we selected a representative subset from the MARIOEval benchmark (Chen et al. 2024a) for comprehensive testing and analysis.

Evaluation Metrics and Baselines

The experiments employ five metrics: Word Accuracy and Normalized Edit Distance (NED) (Tuo et al. 2024) are employed to evaluate the accuracy of text rendering. CLIP-Score (Hessel et al. 2021), VQAScore (Lin et al. 2024), and Aesthetics (LAION-AI 2022) are utilized to assess the quality of the generated images. For detailed configurations of the metrics calculation, please refer to the supplementary materials. We compare our method on CVTG-2K with state-of-the-art Text-to-Image models including Stable Diffusion 3.5 Large (Esser et al. 2024), FLUX.1 dev. To highlight the distinction between CVTG and multi-line text generation, we compare with methods capable of generating multi-line text, such as AnyText (Tuo et al. 2024) and TextDiffuser2 (Chen et al. 2025). To highlight the difference between CVTG and multi-instance generation, we also compare with methods like RAG-Diffusion (Chen et al. 2024b) and 3DIS (Zhou et al. 2025b). Given that the MARIOEval benchmark exclusively comprises single visual text prompts without multi-instance configurations, we excluded RAG-Diffusion and 3DIS from the MARIOEval evaluation. Accordingly, AnyText and TextDiffuser serve as representative visual text generation baselines for MARIOEval evaluation.

The parameter $\lambda = 0.4$ described in Instance Fusion, and $r = 5$ in Region Insulation. Each baseline is run once on

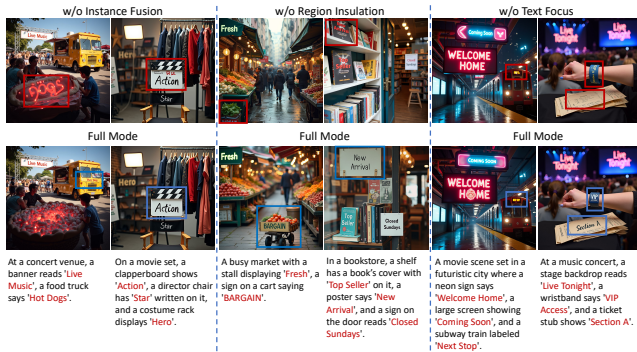


Figure 7: **Qualitative results of ablation studies on each step individually.** The incorrectly rendered visual text is highlighted with a red box, while the corresponding correctly rendered visual text is highlighted with a blue box.

each data sample. Notably, TextCrafter is compatible with different DiT backbone networks, and we have implemented versions with both FLUX.1 and Stable Diffusion 3. All experiments can be completed on a *single* A6000 GPU. For specific data on memory utilization and computational runtime, please refer to the supplementary materials.

Quantitative Results

As demonstrated in Table 2, TextCrafter surpasses competing methods in both text accuracy and image quality on CVTG-2K, with TextCrafter (FLUX) improving word accuracy by over 45% relative to FLUX. While Stable Diffusion 3.5 and FLUX perform adequately in simple scenarios, their efficacy diminishes significantly with increased textual complexity. AnyText and TextDiffuser-2, despite being trained on rule-based data, fail to generalize to multi-region tasks. Similarly, RAG-Diffusion and 3DIS struggles with visual text generation despite its multi-instance capabilities. While TextCrafter was not originally designed for single visual text scenarios, it nevertheless achieves the highest text rendering accuracy and aesthetic quality on established benchmarks such as MARIOEval while maintaining superior instruction-following capability, as shown in Table 3.

As a training-free approach, TextCrafter maintains superior aesthetic scores while balancing textual accuracy with visual coherence, demonstrating exceptional robustness across complexity levels. Comprehensive results are available in the supplementary material.

Qualitative Results

Figure 6 illustrates comparative visual results between TextCrafter and state-of-the-art models on CVTG-2K. While SD3.5 and FLUX generate visually appealing images, they exhibit deficiencies in text rendering as regional complexity increases. AnyText demonstrates suboptimal performance with multi-word text instances, TextDiffuser-2 compromises background fidelity (resulting in diminished CLIP-Score), and 3DIS deteriorates textual information during layout-to-depth conversion. While RAG-Diffusion excels at region-aware generation, it tends to neglect the rendering of

visual text. Conversely, TextCrafter achieves superior visual harmony while accurately rendering multiple text regions without attribute confusion or prompt deviation. To further validate the effectiveness, we conducted a user study with experienced image generation researchers, with detailed results provided in the supplementary material.

Ablation Study

Table 4 presents quantitative ablation results for individual and combined components. Figure 7 shows the qualitative results of missing a step and full mode.

Instance Fusion. Disabling Instance Fusion minimally impacts overall metrics but is vital for correct visual text localization; its absence often leads to misplaced text (*e.g.*, “Hot Dogs” Figure 7, first column). Enabling it also suppresses hallucinated text (*e.g.*, Figure 7, second column). Despite an apparent performance drop when applied alone (Word Accuracy from 0.4965 to 0.4422), the model with all three components enabled still reaches state-of-the-art, emphasizing the progressive and synergistic role of Instance Fusion within the complete pipeline.

Region Insulation. Enabling Region Insulation improves all metrics by decoupling complex visual text, thereby reducing CVTG complexity and maximizing pre-trained model utility. It achieves over 60% word accuracy independently and reduces inter-text interference, enhancing clarity (*e.g.*, “Arrival”, Figure 7, fourth column).

Text Focus. Text Focus offers the most significant metric improvement, especially for small visual text (*e.g.*, “Next Stop” and “VIP Access”, Figure 7, fifth and last columns). Alone, it yields 63.51% word accuracy, roughly 10% below optimal, indicating a need for Instance Fusion and Region Insulation for stability in complex scenarios.

Layout Optimizer Effectiveness. The proposed Manhattan distance-based layout optimizer significantly influences final generation by creating non-overlapping bounding boxes aligned with pretrained models’ spatial preferences. Table 4 quantitatively demonstrates its superiority over alternatives like Random or Fixed Layouts.

Conclusion

This paper addresses complex visual text generation (CVTG) by proposing TextCrafter, a novel training-free framework built on the DiT model. It employs step-by-step refinement from prompts to clauses and finally to specific visual text. Key innovations include Instance Fusion for text-spatial carrier linkage, Region Insulation to reduce complexity and text omission, and Text Focus for accurate small-text rendering. A new CVTG-2K benchmark dataset is also introduced. Extensive experiments demonstrate TextCrafter’s significant advantages over existing methods.

Limitations TextCrafter is constrained by the generative capabilities of the base models and does not support visual text generation in languages other than English. We plan to address this limitation in future research.

References

- BlackForest. 2024. Black Forest Labs; Frontier AI Lab.
- Cai, M.; Cun, X.; Li, X.; Liu, W.; Zhang, Z.; Zhang, Y.; Shan, Y.; and Yue, X. 2024. DiTCtrl: Exploring Attention Control in Multi-Modal Diffusion Transformer for Tuning-Free Multi-Prompt Longer Video Generation. *arXiv preprint arXiv:2412.18597*.
- Chefer, H.; Alaluf, Y.; Vinker, Y.; Wolf, L.; and Cohen-Or, D. 2023. Attend-and-excite: Attention-based semantic guidance for text-to-image diffusion models. *ACM Transactions on Graphics (TOG)*, 42(4): 1–10.
- Chen, J.; Huang, Y.; Lv, T.; Cui, L.; Chen, Q.; and Wei, F. 2024a. Textdiffuser: Diffusion models as text painters. *Advances in Neural Information Processing Systems*, 36.
- Chen, J.; Huang, Y.; Lv, T.; Cui, L.; Chen, Q.; and Wei, F. 2025. Textdiffuser-2: Unleashing the power of language models for text rendering. In *European Conference on Computer Vision*, 386–402. Springer.
- Chen, Z.; Gao, R.; Xiang, T.-Z.; and Lin, F. 2023. Diffusion model for camouflaged object detection. In *ECAI 2023*, 445–452. IOS Press.
- Chen, Z.; Li, Y.; Wang, H.; Chen, Z.; Jiang, Z.; Li, J.; Wang, Q.; Yang, J.; and Tai, Y. 2024b. Region-aware text-to-image generation via hard binding and soft refinement. *arXiv preprint arXiv:2411.06558*.
- Dhariwal, P.; and Nichol, A. 2021. Diffusion models beat gans on image synthesis. *Advances in neural information processing systems*, 34: 8780–8794.
- Esser, P.; Kulal, S.; Blattmann, A.; Entezari, R.; Müller, J.; Saini, H.; Levi, Y.; Lorenz, D.; Sauer, A.; Boesel, F.; et al. 2024. Scaling rectified flow transformers for high-resolution image synthesis. In *Forty-first International Conference on Machine Learning*.
- Feng, W.; He, X.; Fu, T.-J.; Jampani, V.; Akula, A. R.; Narayana, P.; Basu, S.; Wang, X. E.; and Wang, W. Y. 2022. Training-Free Structured Diffusion Guidance for Compositional Text-to-Image Synthesis. In *The Eleventh International Conference on Learning Representations*.
- Hertz, A.; Mokady, R.; Tenenbaum, J.; Aberman, K.; Pritch, Y.; and Cohen-or, D. 2022. Prompt-to-Prompt Image Editing with Cross-Attention Control. In *The Eleventh International Conference on Learning Representations*.
- Hessel, J.; Holtzman, A.; Forbes, M.; Le Bras, R.; and Choi, Y. 2021. CLIPScore: A Reference-free Evaluation Metric for Image Captioning. In *Proceedings of the 2021 Conference on Empirical Methods in Natural Language Processing*, 7514–7528.
- Ho, J.; Jain, A.; and Abbeel, P. 2020. Denoising diffusion probabilistic models. *Advances in neural information processing systems*, 33: 6840–6851.
- Hu, T.; Li, L.; van de Weijer, J.; Gao, H.; Khan, F. S.; Yang, J.; Cheng, M.-M.; Wang, K.; and Wang, Y. 2024. Token Merging for Training-Free Semantic Binding in Text-to-Image Synthesis. *arXiv preprint arXiv:2411.07132*.
- Ji, J.; Zhang, G.; Wang, Z.; Hou, B.; Zhang, Z.; Price, B. L.; and Chang, S. 2023. Improving Diffusion Models for Scene Text Editing with Dual Encoders. *Transactions on Machine Learning Research*.
- LAION-AI. 2022. LAION-Aesthetics Predictor V1.
- Li, Y.; Liu, H.; Wu, Q.; Mu, F.; Yang, J.; Gao, J.; Li, C.; and Lee, Y. J. 2023. Gligen: Open-set grounded text-to-image generation. In *Proceedings of the IEEE/CVF Conference on Computer Vision and Pattern Recognition*, 22511–22521.
- Lin, Z.; Pathak, D.; Li, B.; Li, J.; Xia, X.; Neubig, G.; Zhang, P.; and Ramanan, D. 2024. Evaluating text-to-visual generation with image-to-text generation. In *European Conference on Computer Vision*, 366–384. Springer.
- Liu, Z.; Liang, W.; Liang, Z.; Luo, C.; Li, J.; Huang, G.; and Yuan, Y. 2025. Glyph-byt5: A customized text encoder for accurate visual text rendering. In *European Conference on Computer Vision*, 361–377. Springer.
- Ma, J.; Zhao, M.; Chen, C.; Wang, R.; Niu, D.; Lu, H.; and Lin, X. 2023. GlyphDraw: Seamlessly Rendering Text with Intricate Spatial Structures in Text-to-Image Generation. *arXiv preprint arXiv:2303.17870*.
- OpenAI. 2024. O1Mini: Advancing Cost-Efficient Reasoning.
- Peebles, W.; and Xie, S. 2023. Scalable diffusion models with transformers. In *Proceedings of the IEEE/CVF International Conference on Computer Vision*, 4195–4205.
- Podell, D.; English, Z.; Lacey, K.; Blattmann, A.; Dockhorn, T.; Müller, J.; Penna, J.; and Rombach, R. 2023. SDXL: Improving Latent Diffusion Models for High-Resolution Image Synthesis. In *The Twelfth International Conference on Learning Representations*.
- Ramesh, A.; Dhariwal, P.; Nichol, A.; Chu, C.; and Chen, M. 2022. Hierarchical text-conditional image generation with clip latents. *arXiv preprint arXiv:2204.06125*, 1(2): 3.
- Ramesh, A.; Pavlov, M.; Goh, G.; Gray, S.; Voss, C.; Radford, A.; Chen, M.; and Sutskever, I. 2021. Zero-shot text-to-image generation. In *International conference on machine learning*, 8821–8831. Pmlr.
- Rombach, R.; Blattmann, A.; Lorenz, D.; Esser, P.; and Ommer, B. 2022. High-resolution image synthesis with latent diffusion models. In *Proceedings of the IEEE/CVF conference on computer vision and pattern recognition*, 10684–10695.
- Tumanyan, N.; Geyer, M.; Bagon, S.; and Dekel, T. 2023. Plug-and-play diffusion features for text-driven image-to-image translation. In *Proceedings of the IEEE/CVF Conference on Computer Vision and Pattern Recognition*, 1921–1930.
- Tuo, Y.; Xiang, W.; He, J.-Y.; Geng, Y.; and Xie, X. 2024. AnyText: Multilingual Visual Text Generation and Editing. In *The Twelfth International Conference on Learning Representations*.
- Wei, J.; Wang, X.; Schuurmans, D.; Bosma, M.; Xia, F.; Chi, E.; Le, Q. V.; Zhou, D.; et al. 2022. Chain-of-thought prompting elicits reasoning in large language models. *Advances in neural information processing systems*, 35: 24824–24837.

Xie, J.; Li, Y.; Huang, Y.; Liu, H.; Zhang, W.; Zheng, Y.; and Shou, M. Z. 2023. Boxdiff: Text-to-image synthesis with training-free box-constrained diffusion. In *Proceedings of the IEEE/CVF International Conference on Computer Vision*, 7452–7461.

Yang, L.; Yu, Z.; Meng, C.; Xu, M.; Ermon, S.; and Bin, C. 2024a. Mastering text-to-image diffusion: Recaptioning, planning, and generating with multimodal llms. In *Forty-first International Conference on Machine Learning*.

Yang, Y.; Gui, D.; Yuan, Y.; Liang, W.; Ding, H.; Hu, H.; and Chen, K. 2024b. Glyphcontrol: Glyph conditional control for visual text generation. *Advances in Neural Information Processing Systems*, 36.

Zhang, H.; Hong, D.; Gao, T.; Wang, Y.; Shao, J.; Wu, X.; Wu, Z.; and Jiang, Y.-G. 2024a. CreatiLayout: Siamese Multimodal Diffusion Transformer for Creative Layout-to-Image Generation. *arXiv preprint arXiv:2412.03859*.

Zhang, L.; Chen, X.; Wang, Y.; Lu, Y.; and Qiao, Y. 2024b. Brush your text: Synthesize any scene text on images via diffusion model. In *Proceedings of the AAAI Conference on Artificial Intelligence*, volume 38, 7215–7223.

Zhangli, Q.; Jiang, J.; Liu, D.; Yu, L.; Dai, X.; Ramchandani, A.; Pang, G.; Metaxas, D. N.; and Krishnan, P. 2024. Layout-agnostic scene text image synthesis with diffusion models. In *2024 IEEE/CVF Conference on Computer Vision and Pattern Recognition (CVPR)*, 7496–7506. IEEE Computer Society.

Zhao, C.; Cai, W.; Dong, C.; and Hu, C. 2024. Wavelet-based fourier information interaction with frequency diffusion adjustment for underwater image restoration. In *Proceedings of the IEEE/CVF Conference on Computer Vision and Pattern Recognition*, 8281–8291.

Zhao, Y.; and Lian, Z. 2025. Udifftext: A unified framework for high-quality text synthesis in arbitrary images via character-aware diffusion models. In *European Conference on Computer Vision*, 217–233. Springer.

Zheng, G.; Zhou, X.; Li, X.; Qi, Z.; Shan, Y.; and Li, X. 2023. Layoutdiffusion: Controllable diffusion model for layout-to-image generation. In *Proceedings of the IEEE/CVF Conference on Computer Vision and Pattern Recognition*, 22490–22499.

Zhou, D.; Li, M.; Yang, Z.; and Yang, Y. 2025a. DreamRenderer: Taming Multi-Instance Attribute Control in Large-Scale Text-to-Image Models. *arXiv preprint arXiv:2503.12885*.

Zhou, D.; Li, Y.; Ma, F.; Zhang, X.; and Yang, Y. 2024. Mige: Multi-instance generation controller for text-to-image synthesis. In *Proceedings of the IEEE/CVF Conference on Computer Vision and Pattern Recognition*, 6818–6828.

Zhou, D.; Xie, J.; Yang, Z.; and Yang, Y. 2025b. 3dis: Depth-driven decoupled instance synthesis for text-to-image generation. In *The Twelfth International Conference on Learning Representations*.